Supplementary Information

Three-dimensional "Skin-Framework" Hybrid Network as Electroactive Material Platform for High-Performance Solid-state Asymmetric Supercapacitor

Liaoyuan Xia, [a, b*] Shaoheng Hu, [a, b] Xueqin Zhang,[a, b] Le Huang, [a] Yu Liao, [a] Yan Qing, [a] Yiqiang Wu, [a*] Wenping Jiang,[a] and Xihong Lu [c*]

[a] College of Material Science and Engineering, Central South University of Forestry and Technology, Changsha 410004, P. R. China. E-mail: wuyq0506@126.com

[b] Hunan Province Key Laboratory of Materials Surface & Interface Science and Technology, Central South University of Forestry and Technology, Changsha 410004, P. R. China. E-mail: xly1516@126.com

[c] MOE of the Key Laboratory of Bioinorganic and Synthetic Chemistry, School of Chemistry, Sun Yat-Sen University, Guangzhou 510275, P. R. China. E-mail: luxh6@mail.sysu.edu.cn

S1. Calculations

1. 1. Calculation of the areal specific capacitance of the single electrode

(1) The areal specific capacitance of the electrodes was calculated from the CV curves using Equation (1):

$$C_a = \frac{Q}{\Delta U \times S} \qquad (1)$$

where C_a (mF/cm^2) is the areal specific capacitance, Q is the average charge during electrode charging and discharging, ΔU (V) is the working voltage window of the electrode, and S (cm^2) is the test area of the electrodes.

(2) C_a was calculated by galvanostatic charging-discharging using Equation (2):

$$C_a = \frac{I \times \Delta t}{\Delta U \times S} \qquad (2)$$

where I is the current during electrode discharging (A), and Δt (s) is the DC discharge time of the electrode.

(3) The mass specific capacitance with respect to the three-electrode configuration was derived from galvanostatic charging-discharging based on Equations (3) and (4):

$$C_s = \frac{Q(MnO_2 + MWCNT) - Q(MWCNT)}{\Delta U_1 \times m_1} \qquad (3)$$

$$C_s = \frac{Q(AC + MWCNT) - Q(MWCNT)}{\Delta U_2 \times m_2} \qquad (4)$$

where C_s is the mass specific capacitance, Q is the charge obtained from the galvanostatic charging-discharging based on the MnO_2-MCN, AC-MCN and MCN electrodes, ΔU_1 (=0.8 V) and ΔU_2 (=1.0 V) constitute the voltage range, m_1 is the mass of MnO_2 loaded on the MnO_2-

MCN electrode, and m_2 is the mass of AC loading on the AC-MCN electrode.

1. 2. Calculation of volume specific capacitance, power density, and energy density of the MnO_2-MCN//AC-MCN solid-state ASC device

(1) The volume specific capacitance of the electrodes was calculated from the CV curves and from Equations (5) and (6):

$$C_{cell} = \frac{Q}{\Delta U} \qquad (5)$$

$$C_V = \frac{C_{cell}}{V} = \frac{Q}{V \times \Delta U} \qquad (6)$$

where C_{cell} is the capacitance and CV is the volume specific capacitance of the device, Q is the average charge during electrode charging and discharging, ΔU (V) is the working voltage window of the device. V (cm^3) is the volume of the device, including the volumes of the positive and negative electrode pieces, gel electrolyte, and diaphragm. The area, thickness, and volume of the MnO_2-MCN//AC-MCN solid-state ASC device were 1.0 cm^2, 521 μm (see Fig. S9), and 0.521 cm^3, respectively.

(2) The specific capacitance of the device was calculated from the discharging curve using Equations (7) and (8):

$$C_{cell} = \frac{I \times \Delta t}{\Delta U} \qquad (7)$$

$$C_s = \frac{C_{cell}}{m} = \frac{I \times \Delta t - C_{MWCNT} m_{MWCNT}}{m \times \Delta U} \qquad (8)$$

where C_{cell} is the capacitance and C_s is the mass specific capacitance of the device; I is the

current during the device discharging (A), and Δt (s) is the DC discharge time of the device; ΔU (V) is the working voltage window of the device; m (g) is the mass of the active material, where m includes the MnO_2 and AC.

(3) Equations (9)–(11) were used to calculate the energy density (E, mWh/cm^3), equivalent series resistance (ESR, i.e., the internal resistance of the capacitor, Ω), and power density (P, mW/cm^3) of the device, respectively:

$$E = \frac{1}{2\times 3600} C_V \Delta U^2 \qquad (9)$$

$$ESR = \frac{iR_{drop}}{2\times I} \qquad (10)$$

$$P = \frac{\Delta U^2}{4\times ESR\times V} \qquad (11)$$

where C_v is the volume specific capacitance of the device, ΔU (V) is the working voltage window, and iR_{drop} is the voltage drop.

S2. Various graphs and curves

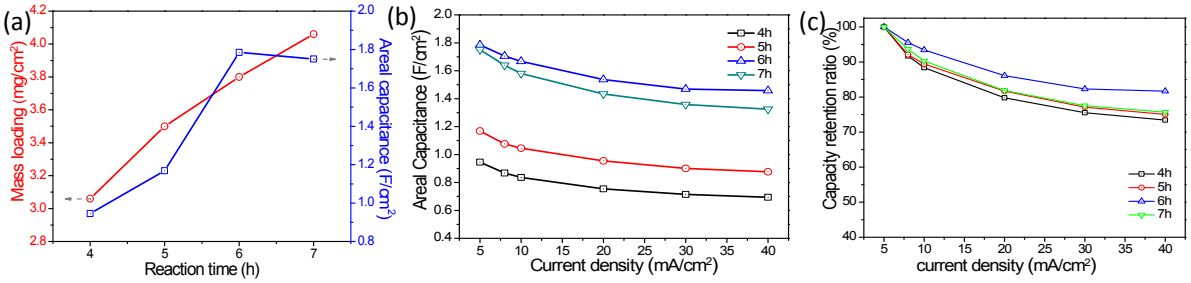

Fig. S1 (a) Mass loading and areal specific capacitance of the MnO_2-MCN electrode as a function of reaction times; (b) areal capacitance; and (c) capacitance retention rate of the MnO_2-MCN electrode as functions of the current density.

As expected, and as shown in Fig. S1a, when MCN is used as the active material platform, the mass loading of MnO_2 increases proportionally with the reaction time. However, the areal specific capacity of the MnO_2-MCN electrode initially increases and then decreases with time. This is because MnO_2 nanoparticles substantially aggregates on the MWCNT surface with increasing the reaction time, with adverse effects on the electrochemical performance of the MnO_2-MCN electrode. Fig. S1b and c show the electrodes area specific capacity and capacity retention as a function of current density at different times. Obviously, the MnO_2-MCN electrode prepared with reaction time for 6h has a larger area specific capacity and a better capacity retention. The experimental results thus indicate an optimal reaction time of 6h, and this was adopted for further electrochemical investigation in this work.

Fig. S2 Display of large-scale preparation of the MCN hybrid materials.

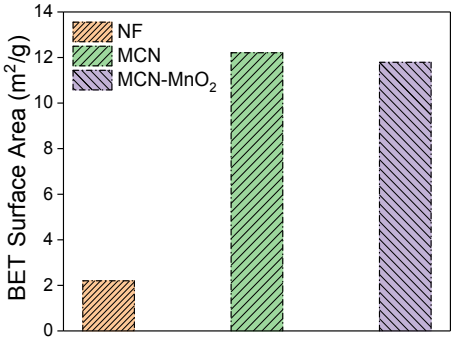

Fig. S3 Histogram of the specific surface area of the NF, MCN, and MnO_2-MCN electrode materials.

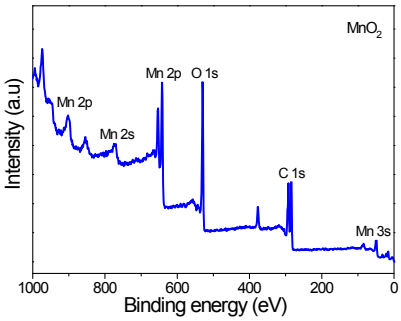

Fig. S4 XPS full spectra of the MnO_2-MCN electrode.

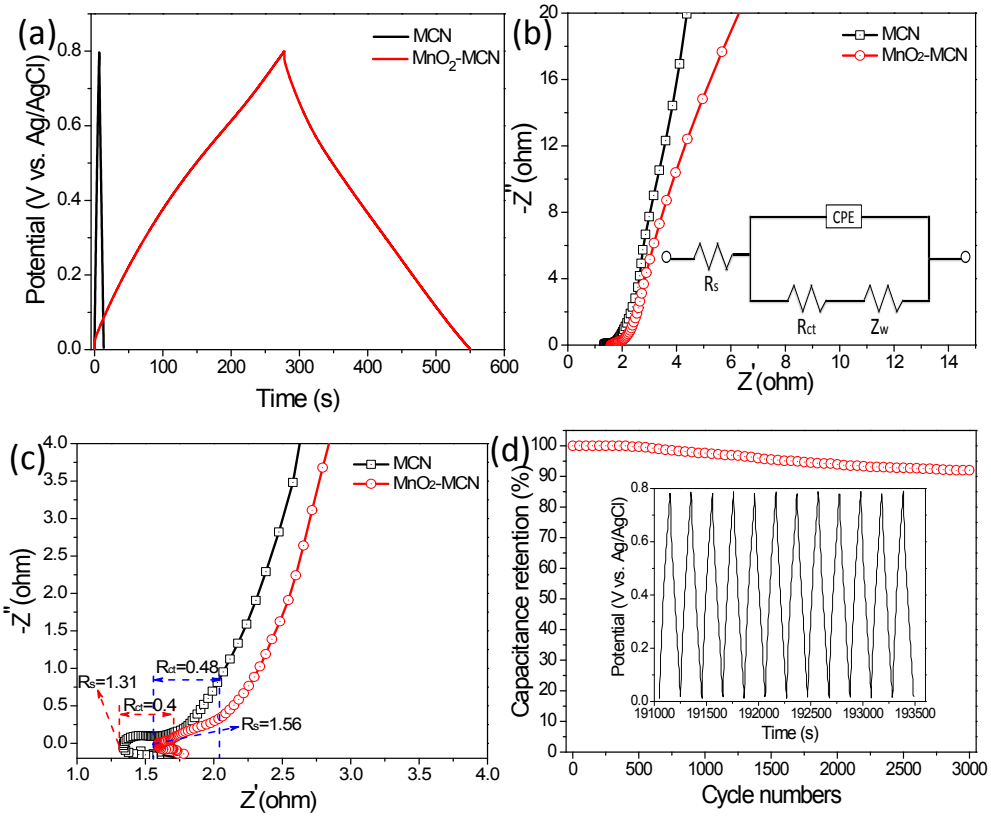

Fig. S5 (a) GCD curves of the MCN and MnO_2-MCN electrodes collected at a current density of 5 mA/cm^2; (b) Nyquist plots of the MCN and MnO_2-MCN electrodes with the equivalent circuit diagram used for fitting the EIS data (inset); (c) Nyquist plots of the

MCN and MnO_2-MCN electrodes with the corresponding high-frequency parts; and (d) cycle performance of the MnO_2-MCN electrode at current density of 10 mA/cm^2.

As shown in Fig. S5 (b), the equivalent circuit diagram used for the fitting of the EIS data includes the equivalent series resistance (R_s), the charge transfer resistance (R_{ct}), the diffusion impedance (Z_w), and the constant phase element (CPE) to account for the double layer capacitance. It is seen that the MCN electrode had smaller R_s and R_{ct} compared with the MnO_2-MCN electrode.This mainly attributed to the poor electronic conductivity of nano-MnO_2 (1×10^{-5} to 1×10^{-6} S/cm) loaded onto the MCN platform, resulting in a large R_{ct} of the MnO_2-MCN electrode. Further, when the MnO_2 nanoparticles was loaded, the insufficiently developed porous structure of the MnO_2-MCN electrode combined with the poor liquid absorption ability led to the increase in the Z_w of the MnO_2-MCN electrode to become large.

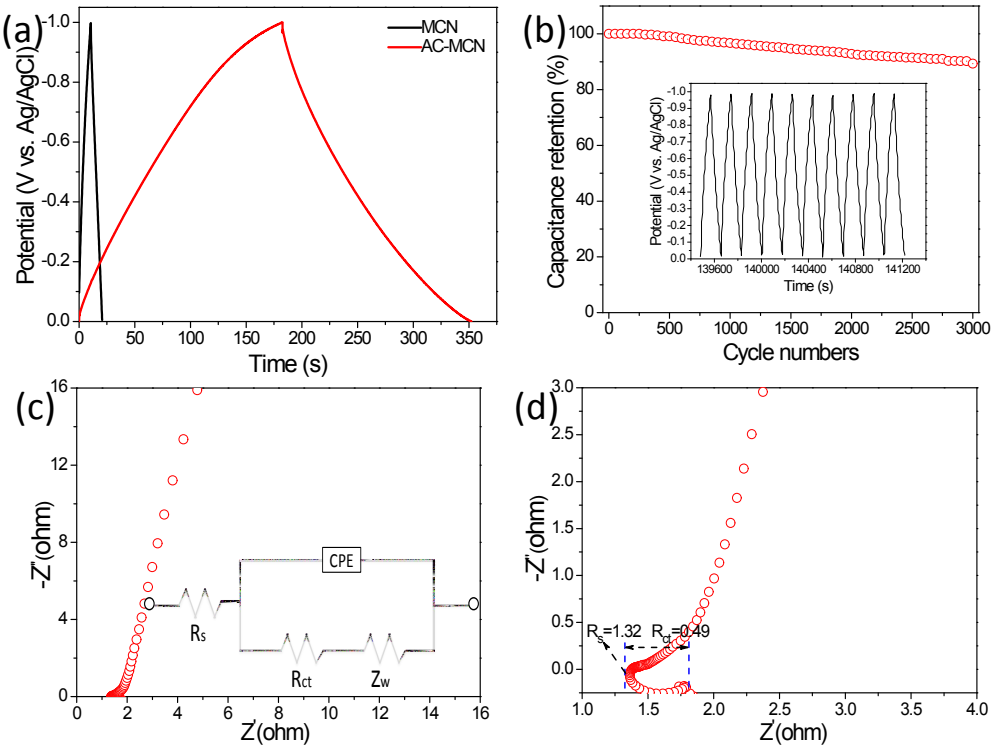

Fig. S6 (a) GCD curves of the MCN and AC-MCN electrodes collected at a current density of 5 mA/cm^2; (b) cycle performance of the AC-MCN electrode at a current density of 10 mA/cm^2; (c) Nyquist plots of the AC-MCN electrode with the equivalent circuit

diagram used for fitting the EIS data (inset); and (d) Nyquist plots of the AC-MCN electrode with the corresponding high-frequency part.

The equivalent circuit diagram used for the fitting of the EIS data is presented in inset of Fig. S6 (c), which includes the equivalent series resistance (R_s), the charge transfer resistance (R_{ct}), the diffusion impedance (Z_w), and the constant phase element (CPE) to account for the double layer capacitance. As shown in Fig. S6 (d), It can be seen that the AC-MCN electrode had a low R_s (1.32 Ω) and R_{ct} (0.49Ω).This mainly attributed to the good electronic conductivity of MCN electroactive platform.

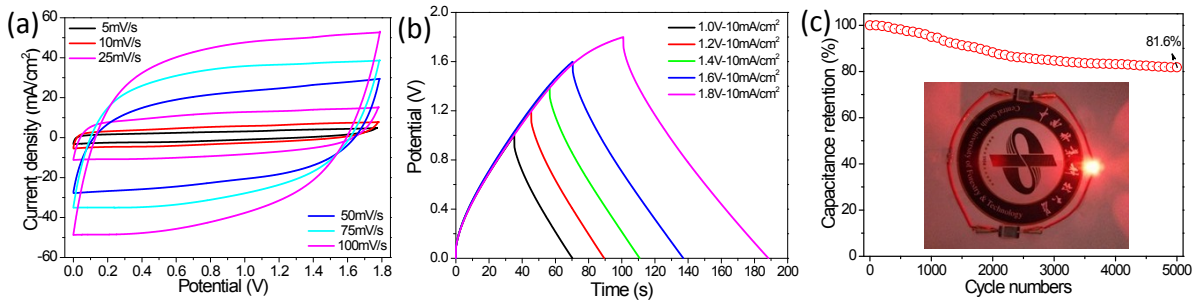

Fig. S7 (a) CV curves of the MnO_2-MCN//AC-MCN solid-state ASC device collected at scan rates of 5–100 mV/s; (b) GCD curves of the ASC device within various operation voltage windows at a current density of 10 mA/cm^2; and (c) cycle performance of the MnO_2-MCN//AC-MCN solid-state ASC device and (inset) photograph of an LED indicator (3 V) powered by two 1 cm × 1 cm units of the ASC device in series.

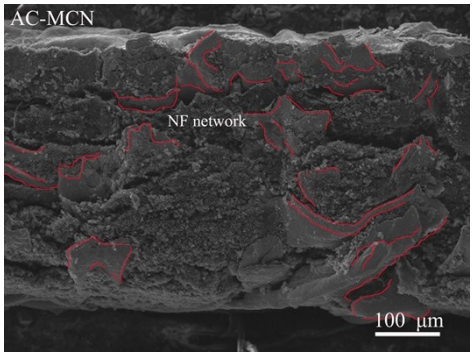

Fig. S8 Cross-sectional SEM image of the AC-MCN electrode sheet.

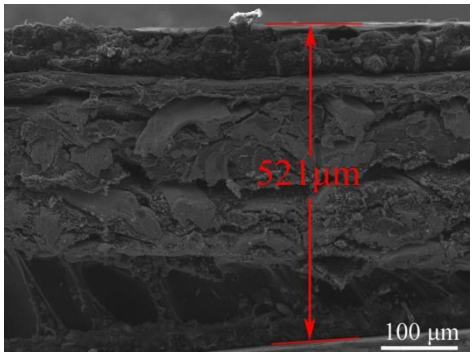

Fig. S9 Cross-sectional SEM image of the MnO_2-MCN//AC-MCN solid-state ASC device.

S3. Video

Video S1 Demonstration of the structural stability of the MWCNT/CNF "skin" in the MCN platform by ultrasonic treatment.

Video S2 Demonstration of the good wettability of the MCN, MnO_2-MCN and AC-MCN electrodes.